

Nitric and nitrous oxide emissions following fertilizer application to agricultural soil: Biotic and abiotic mechanisms and kinetics

Rodney T. Venterea¹ and Dennis E. Rolston

Department of Land, Air, and Water Resources, University of California, Davis

Abstract. Emissions of nitric and nitrous oxide (NO and N₂O) from agricultural soils may have several consequences, including impacts on local tropospheric and global stratospheric chemistry. Elevated NO and N₂O emissions following application of anhydrous ammonia to an agricultural field in California were driven by the biological generation of nitrite (NO₂⁻) and subsequent abiotic decomposition of nitrous acid (HNO₂). Maximum fluxes of > 1000 ng NO-N cm⁻² h⁻¹ and > 400 ng N₂O-N cm⁻² h⁻¹ were observed, and emissions of > 100 ng NO-N cm⁻² h⁻¹ and > 50 ng N₂O-N cm⁻² h⁻¹ persisted for > 4 weeks. Laboratory experiments were performed to determine rate coefficients and activation energies for HNO₂-mediated NO and N₂O production. Kinetic parameters describing the conversion of NO to N₂O were measured and were found to vary with water-filled pore space (WFPS). Regression models incorporating HNO₂, WFPS, and temperature accounted for 75–77% of the variability in field fluxes. A previously developed NO emissions model was modified to incorporate a kinetic expression for HNO₂- and temperature-dependent production. The model tended to underestimate fluxes under low-flux conditions and overestimate fluxes under high-flux conditions. These data indicate that (1) control of acidity may be an effective means for minimizing gaseous N losses from fertilized soils and possibly for improving air quality in rural areas, (2) the transformation of HNO₂-derived NO may be an important mechanism of N₂O production even under relatively aerobic conditions, and (3) mechanistic models which account for spatial heterogeneity and transient conditions may be required to better predict field NO fluxes.

1. Introduction

Agricultural soils have been recognized as a significant source of nitric and nitrous oxide, which are important trace gases involved in several critical processes in the atmosphere [Veldkamp and Keller, 1997a; Davidson, 1991]. Nitric oxide (NO) is a precursor to nitric acid and plays a central role in photochemical reactions which regulate levels of tropospheric ozone (O₃) [Crutzen, 1979, 1981]. Because tropospheric NO tends to limit rates of O₃-forming reactions in rural areas, soil emissions have the potential to significantly impact local O₃ levels [Stohl *et al.*, 1996]. With the recent promulgation of new ambient air quality standards for O₃ in the United States, there is increasing concern regarding air quality violations in rural areas [Saylor *et al.*, 1998]. Ozone can have detrimental effects on plants upon extended exposure to levels as low as 40 nL L⁻¹ [Holopainen, 1996] and is believed to be responsible for crop losses of more than \$2 billion yr⁻¹ in the United States

[Delucchi *et al.*, 1996]. Nitrogen dioxide (NO₂), which forms rapidly from oxidation of NO, can have synergistic phytotoxic effects in combination with O₃ and/or sulfur dioxide [Heck, 1989]. The release of NO from agricultural soil can also result in losses of 5–10% of applied fertilizer nitrogen (N) [Shepherd *et al.*, 1991; Veldkamp and Keller, 1997a, b]. Nitrous oxide (N₂O) accounts for an estimated 5% of the total anthropogenic greenhouse effect [Rodhe, 1990] and is increasing in the atmosphere at about 0.25% yr⁻¹ [Prinn *et al.*, 1990]. The oxidation of N₂O to NO in the stratosphere promotes O₃ destruction [Crutzen, 1981]. There is a recognized need for improved understanding of the factors responsible for high variabilities observed in measurements of NO and N₂O emissions from soils [Matson, 1997; Mosier *et al.*, 1996] in order to reduce uncertainties in global budgeting efforts [Davidson and Kingler, 1997] and to aid in the development of strategies for mitigating N losses from intensively fertilized agricultural systems [Matson *et al.*, 1998].

NO and N₂O are produced during the transformation of soil N by the microbial processes of nitrification and denitrification and from abiotic reactions [Firestone and Davidson, 1989]. Abiotic mechanisms involve nitrite (NO₂⁻), produced by nitrification and/or denitrification, which is protonated to form nitrous acid (HNO₂) at low pH (pK_a = 3.3) [Van Cleemput and Samater, 1996]. Nitrous acid can subsequently decompose in

¹Now at Institute of Ecosystem Studies, Millbrook, New York.

aqueous solution to form NO [Pauling, 1970] and/or react nonenzymatically with soil constituents to form NO and N₂O [Nelson, 1982]. While these abiotic processes have been recognized for several decades [Reuss and Smith, 1965], most studies have been conducted under laboratory conditions [Smith and Chalk, 1980; Blackmer and Cerrato, 1986; McKenney et al., 1990]. Recent laboratory experiments have demonstrated that gross NO production rates in sterile and nonsterile agricultural soils were highly correlated with HNO₂ concentrations but were not correlated with gross nitrification rates or other N substrate levels (i.e., NH₄⁺ or NO₃⁻) [Venterea and Rolston, 2000]. The potential importance of HNO₂-mediated reactions in the field has been suggested by laboratory experiments accompanying field measurement of NO emissions [Serca et al., 1994] and measurements of high NO₂⁻ concentrations corresponding to peak NO field fluxes [Davidson et al., 1991].

Anhydrous ammonia (AA) is one of the most commonly used agricultural N fertilizers in the United States, Canada and Australia [Stehouwer and Johnson, 1990; Strong and Cooper, 1992; Bouman et al., 1995; California Department of Food and Agriculture, 1998]. The accumulation of NO₂⁻ has been observed following the application of AA, which is rapidly hydrolyzed in water resulting in increased pH [Chalk et al., 1975; Van Cleemput and Samater, 1996]. Subsequent lowering of soil pH by as much as four units can occur due to nitrification of NH₄⁺, which can reach concentrations > 1000 µg N g soil⁻¹ near points of fertilizer application [Frederick and Broadbent, 1965]. Although pH values may return to near-initial levels in the short term, more persistent acidification can be promoted by continued fertilizer use over several years [Bouman et al., 1995]. In acid-to-neutral soils which continue to receive intensive N inputs, the accumulation of NO₂⁻ following fertilizer application may create optimum conditions for localized HNO₂ formation and NO production, as proposed by Nelson [1982]. While the production of N₂O directly from HNO₂-mediated reactions may be relatively insignificant compared to HNO₂-mediated NO production [Bremner, 1997; Venterea and Rolston, 2000], microbial transformations of NO to N₂O by denitrifying bacteria have been shown to occur in soils incubated under relatively aerobic conditions [Schafer and Conrad, 1993]. Therefore the objectives of the present study were to (1) examine relationships between localized fluxes of NO and N₂O and levels of HNO₂ in soil directly beneath field gas flux chambers, (2) characterize the HNO₂-mediated kinetics of abiotic NO and N₂O production in the field soil, and (3) examine the potential for NO-mediated N₂O production under bulk aerobic soil conditions.

2. Methods

2.1. HNO₂-Mediated Production Kinetics

Prior to the field experiment, laboratory experiments were initiated in order to examine the potential importance of HNO₂-mediated abiotic NO and N₂O production in this particular soil. Values of the kinetic coefficients relating rates of abiotic NO and N₂O production and HNO₂ concentrations were determined in a field composite using previously established methods in order to establish the order of magnitude of these coefficients and compare them with values previously obtained using three sterilized agricultural soils of similar origin and composition [Venterea and Rolston, 2000]. Another objective was to examine the temperature dependency of the abiotic reactions. A composite field sample comprised of equal portions (1 kg

Table 1. Selected Properties of Field Soil Composite

Parameter	Description or Value
Classification	thermic aquic xerofluvent
Soil series	Columbia loam
Sand, %	51
Silt, %	38
Clay, %	11
Organic C [†] , %	1.1
Total Kjeldahl N, %	0.13
CEC [‡] , µeq g ⁻¹	120
Soil pH	5.3 (1:1 H ₂ O)
	5.1 (1:1 1 M KCl)

[†]Dichromate oxidation.

[‡]Cation exchange capacity.

each) of individual samples was collected from the top 0-10 cm at 10 locations distributed in a grid pattern across the 2.5-ha field in September of 1997 prior to harvest. Selected properties of the field composite sample are shown in Table 1. Separate 300-g portions (stored at 4°C) of the composite sample were air dried and sieved (2 mm) and then adjusted to pH values of 6.6, 5.3 (no adjustment), 4.8, and 4.1. Each portion was exposed to 3-5 Mrad of λ radiation (at Phoenix Memorial Laboratories, University of Michigan, Ann Arbor). Replicate subsamples (5-20 g each) at each pH were amended with aqueous solutions of KNO₂, followed immediately by measurement of NO₂⁻ concentration, pH, and gross NO and/or N₂O production rate, as previously described [Venterea and Rolston, 2000]. For experiments conducted at 25°C, 3-4 levels of KNO₂ concentration were applied at each pH level, with two replications each ($n = 32$ for NO and $n = 24$ for N₂O) (Table 2). For experiments conducted at 20°, 30°, and 35°C, 1 or 2 levels of KNO₂ concentration were applied at each pH level, with two replications each ($n = 10$ for NO and N₂O) (Table 2). All solutions and materials were sterilized by autoclaving or washing with 95% ethanol. Gross NO production rates were determined using a test system based on that of Remde et al. [1989], as described in detail by Venterea and Rolston [2000]. A flow-through cylindrical reaction chamber was used to isolate gross production from consumption, assuming zero-order production and first-order consumption by measuring net production (P_{net}) over varying NO concentrations ($[NO]_e$). Regression of P_{net} versus $[NO]_e$ was used to obtain gross NO production rate (P_{NO}) and first-order consumption rate coefficient (k_c) from

$$P_{net} = P_{NO} - k_c [NO]. \quad (1)$$

For sterile soils, k_c values were immeasurably low ($< 3 \text{ cm}^3 \text{ gas g}^{-1} \text{ soil h}^{-1}$), so P_{NO} values could be accurately determined from P_{net} measured at one level of $[NO]_e$ ($< 0.5 \text{ ng N cm}^{-3}$). Gross N₂O production rates (P_{N2O}) were determined by measurement of N₂O headspace concentrations (typically after 0, 1, and 2 hours) occurring during incubation of samples (3-12 g) in 230-cm³ glass jars equipped with Mininert sampling ports (Dynatech). Consumption of N₂O in sterile soils was assumed to be negligible based on observed linear increases in concentration versus time (r^2 generally > 0.95). Rate coefficients relating gas production rates to HNO₂ concentrations were determined by regression of P_{NO} and P_{N2O} versus HNO₂, that is,

$$P_{NO} = k_{PNO} [HNO_2]^\alpha, \quad (2)$$

Table 2. Design of HNO₂-Mediated Production Kinetics Experiments in Sterile Soil

Soil pH	NO ₂ [†] , μg N g ⁻¹ soil	HNO ₂ [‡] , μg N g ⁻¹ soil
4.1	0.0, 0.7, 1.0 [§] , 1.8	< 0.001, 0.096, 0.137, 0.274
4.8	0.0, 1.5, 4.5, 9.0 [§]	< 0.001, 0.046, 0.138, 0.276
5.3	0.0, 5.0, 10 [§] , 20	< 0.001, 0.050, 0.099, 0.198
6.6	0.0 [§] , 100 [§] , 150, 200	< 0.001, 0.050, 0.075, 0.100

[†]NO₂⁻ treatments shown were used for NO production measurements at 25°C. Treatments within the same concentration ranges were used for N₂O production measurements at 25°C. Approximate added amounts of NO₂⁻ are shown; measured values varied by ± 5%.

[‡]Approximate HNO₂ concentrations are shown; actual values were calculated from measured NO₂⁻ and soil pH values, according to *Venterea and Rolston* [2000].

[§]Approximate levels of NO₂⁻ treatments used for measurements at 20°, 30°, and 35°C.

$$P_{N2O} = k_{PN2O} [HNO_2]^\beta, \quad (3)$$

where α and β are the empirical orders of the overall reactions. Concentrations of HNO₂ were calculated as previously described [*Venterea and Rolston*, 2000] using measured pH and NO₂⁻ concentrations.

2.2. Field Experiment

Field measurements were made during July-August 1998 in a furrow-irrigated tomato field in western Sacramento county, California, comprised of a moderately acidic loam soil. Field measurements were made over the majority of the growing season, with all farming operations managed by a private farmer according to his normal practices. In late June, tomato seedlings were transplanted onto raised beds measuring approximately 140 cm wide, with one row per bed. Several days later, anhydrous ammonia (AA) was injected at a depth of ~15 cm along a line spaced 25-35 cm from each row on both sides at the rate of 120 kg N ha⁻¹. Field measurements were started the day after the first irrigation event, which was on July 2 (referred to as "Day 0"), and continued until August 21 (Day 50). The field was furrow irrigated on three subsequent occasions, July 11, 26, and August 12 (Days 9, 24, and 41), and harvested approximately 2 weeks after the last sampling. No significant rainfall occurred in the week prior to or during the growing season.

2.3. Gas Flux Sampling and Analysis

A total of 135 measurements of NO, N₂O, and CO₂ soil-to-atmosphere flux were made on 19 separate dates (Table 3). On each sampling date, a 100 m² section of the field was randomly selected and gas flux sampling locations were randomly selected from within the AA injection zone of that section (25-35 cm from the row), while maintaining a minimum spacing of 1 m between chambers. Most sampling events were between 1300 and 1500 hours local time (LT). Each location was sampled a single time. A static chamber technique was used to measure gas flux. Thin-walled (0.7 mm) insulated stainless steel cylinders (12.2 cm ID x 13.6 cm) designed in accordance with *Hutchinson and Mosier* [1981] were installed by inserting the base to a depth of 1 cm immediately prior to sample collection. Initial sampling showed that increases in chamber

NO, N₂O, and CO₂ concentrations were linear in time for the first 10-15 min following chamber placement. Subsequent sampling was done at 0, 4-5, 8-10, and/or 12-15 min following placement. Samples for N₂O and CO₂ analysis were removed from chambers with nylon syringes equipped with rubber O-ring plunger seals (Sesi, Cournon D'auvergne, France, number 60350), which were preserved by inserting needles into rubber stoppers until analysis in the laboratory within 3-4 hours. Separate 13 cm³ samples for NO analysis were taken with 30-mL polypropylene syringes (Becton Dickinson) and transferred to 12-cm³ glass Exetainer tubes (Labco) which had been evacuated to < 0.2 torr within the previous 24 hours and sealed with silicone-coated butyl/latex septa. NO sampling syringes were tested to ensure that negligible artifacts resulted from the sampling technique. NO sampling syringes and tubes were kept wrapped in foil to exclude light and were analyzed in the laboratory within 35-60 min.

Concentrations of N₂O were determined by injection of syringe sample into a gas chromatograph (GC) (Hewlett-Packard 6890/⁶³Ni electron capture detector), which was calibrated on each day of sampling using 0.3, 1.5, and 4.5 μL L⁻¹ standards. Concentrations of NO were determined using an O₃-oxidation chemiluminescent NO analyzer, which can be adapted to analyze continuous or discrete samples (Sievers 270B). In discrete mode the limit of NO detection with a 1-cm³ sample is ~ 0.02 ng N cm⁻³ (~ 30 nL L⁻¹), with an analysis time of ~ 30 s per sample. The instrument was calibrated daily using pressurized standards of NO in N₂ which were diluted with air and injected into Exetainer sampling tubes. Instrument response to standards prepared from 10 μL L⁻¹ NO in N₂ pressurized cylinders obtained from two different suppliers varied by < 5% (Scott-Marin and Puritan-Bennet). A gold-catalyzed NO₂ → NO converter (Sievers) was used to check for the presence of NO₂, which was generally below detectable levels (< 100

Table 3. Field Gas Flux and Soil Sampling Schedule

Day of Experiment [†]	Number of Samples	
	Flux Chambers [‡]	Soil Cores [§]
1	6	4
3	6	4
6	6	2
7	6	5
9	6	4
11	6	4
12	9	4
14	6	6
18	6	5
22	6	6
26	6	0
28	8	0
30	9	5
34	9	0
37	9	5
41	9	0
44	4	0
45	9	2
50	9	5
Total	135	61

[†]Samples collected on days 3, 6, 7, 9, 11, 12, and 14 were tested for gross NO production rates and corresponding HNO₂ concentrations in the lab.

[‡]Sampled for NO, N₂O, and CO₂ flux.

[§]Sampled for NH₄⁺, NO₂⁻, NO₃⁻, pH, water content, and temperature at 0-5 and 5-10 cm depths.

nL L⁻¹). Concentrations of CO₂ and O₂ were determined using a GC (Hewlett-Packard 5890/thermal conductivity detector), which was calibrated using pressurized standard gases. Surface fluxes of NO, N₂O, and CO₂ (F_{NO} , F_{N_2O} , F_{CO_2}) were determined from regression of chamber concentrations versus time, chamber volume and cross-sectional area. Ground level O₃ was measured prior to each sampling event using a UV photometric analyzer (Dasibi 1008-H).

Oxidation of NO by O₃ within flux chambers was assumed to be completed within < 4 min, as previously shown [Anderson and Levine, 1987; Hutchinson and Brams, 1992]. Decreases in NO concentrations occurring in sampling tubes over time were measured in tubes containing standards diluted with O₃-free air ($n = 25$) and in field gas flux samples ($n = 15$) collected during the first week of sampling. Measured NO loss rates were compared to theoretical loss rates assuming kinetics for NO oxidation by ambient O₂ using published rate coefficients [Atkinson *et al.*, 1997]. In > 90% of cases, decreases in NO concentration were consistent with theoretical losses. Additional losses of ~ 5% were observed in < 10% of test standards and samples, possibly due to reactions of NO with surfaces or other oxidants. Theoretical losses for field samples, calculated based on time elapsed between sample collection and analysis, were $\geq 5\%$ for a small number of samples ($n = 15$ out of 147) and therefore corrections were not applied to the data. Samples having theoretical losses $\geq 10\%$ ($n = 3$) are noted in the Results. While the static chamber/discrete sampling technique introduces analytical uncertainties, potential interferences associated with dynamic chamber methods are avoided, including the creation of soil-gas advection due to pressurized air circulation [Hutchinson and Mosier, 1981] and errors associated with field instrument calibration [Veldkamp and Keller, 1997b].

2.4. Soil Sample Collection and Analysis

Following 61 of the gas flux measurements (Table 3), soil samples were taken from beneath chamber locations so that relationships could be examined between gas fluxes and soil temperature, water content, inorganic N concentrations, and pH. Soil temperatures at 5 and 10 cm depths were measured within 15 min of flux sampling by insertion of a thermistor/digital thermometer probe adjacent to or within the chamber locations. Soil samples were then collected by insertion of PVC cylinders (15 cm ID x 30 cm) to a depth of 15-20 cm. Cylinders were removed with soil intact, wrapped in plastic and transported to the laboratory. Within 6 hours, soil was removed from the 0-5 cm and 5-10 cm layers, homogenized and transferred to plastic bags which were stored at room temperature until analysis. Within 24 hours (usually within 6 hours) of sample collection, two replicate subsamples (8-20 g each) from each layer were extracted in 0.5 M K₂SO₄ solution by shaking for 60 min. After centrifugation, supernatant was analyzed for total (NO₂⁻ / HNO₂)-N [Keeney and Nelson, 1982; Venterea and Rolston, 2000]. Within 8 days of sample collection, the remainder of the extraction solution (stored at 4°C) was analyzed for NO₃⁻ and NH₄⁺ [Keeney and Nelson, 1982]. Separate individual subsamples (8-12 g) were mixed with an equal mass of 1 M KCl solution, stirred, and allowed to settle for 1 hour before removal of supernatant for pH measurement. Separate individual subsamples (5-20 g) were weighed before and after drying at 105°C for 24 hours for gravimetric water content (θ) determination.

Gross NO production rates and corresponding HNO₂ concentrations were also determined according to methods

described above in nonsterile samples collected from 0-10 cm beneath gas flux chambers during the first 2 weeks of the field experiment (Table 3). These samples were incubated at 25°C and flushed continuously with humidified NO-free air for > 6 hours prior to measurement.

2.5. NO-Mediated N₂O Production Kinetics

Additional laboratory experiments were initiated following the field experiments in order to examine the potential for NO-mediated N₂O production under bulk aerobic conditions at varying levels of water-filled pore space (WFPS) in two separate composite samples. Nonsterile (NS) composite 1 was generated from 100 g each of field samples collected at the 0-5 cm depth beneath six different gas flux chambers sampled on Days 14, 18, and 22. NS composite 2 was generated from 100 g each of field samples collected at the 0-5 cm depth beneath six different gas flux chambers sampled on Days 35, 45, and 50. NS composite 1 contained 110 $\mu\text{g NO}_3^- \text{N g}^{-1}$ and had a pH of 5.0, and NS composite 2 contained 170 $\mu\text{g NO}_3^- \text{N g}^{-1}$ and had a pH of 4.7. NS composite samples 1 and 2 were generated and analyzed 3 months and 15 months following the field experiment, respectively. Samples were stored at room temperature under air-dried conditions. Three separate 100-g portions of each composite were amended with deionized water to achieve WFPS values of 20, 40, and 60%. The portions were incubated for 12 hours in sealed glass jars containing 10 Pa of C₂H₂, which inhibits autotrophic nitrification without affecting denitrification [Davidson *et al.*, 1986]. Nitrification was inhibited in order to limit the number of potential sources of N₂O and to simplify data interpretation. After 12 hours of C₂H₂ exposure, jars were flushed with humidified air for an additional 12 hours. Subsamples (5-15 g) at each WFPS level were then incubated in 230-cm³ jars following the addition of NO to the headspace at concentrations of 0, ~ 2.5, ~ 12, and ~20 ng NO-N cm⁻³ by injecting 5-10 cm³ of 57 or 570 ng NO-N cm⁻³ in N₂ standards (10 cm³ of N₂ was added to the 0-level jars). Each level of WFPS and NO amendment was replicated twice, for a total of 24 jars for each composite (three levels of WFPS, four levels of NO with two replicates of each). Headspace NO concentrations were measured at approximately 30-min intervals, and headspace N₂O concentrations were measured at approximately 1-hour intervals for ~ 2 hours. Headspace O₂ concentrations were ≥ 20 kPa.

3. Results

3.1. HNO₂-Mediated Production Kinetics in Sterile Soils

In sterile (λ irradiated) soils, production of N₂O at 25°C was correlated with HNO₂ ($r^2 = 0.91$, Figure 1a and Table 4). At all temperatures, N₂O production was also correlated ($r^2 = 0.82-0.99$) with HNO₂ concentration, with low relative standard errors (< 10%) for each rate coefficient (k_{PN_2O} , Table 4). Nonlinear regression analysis of the NO production rate data ($n = 32$) at 25°C indicated an apparent reaction order of 1.35 (± 0.06), that is, gross NO production was strongly correlated ($r^2 = 0.95$) with HNO₂^{1.35} (Figure 1a). Gross NO production rates at 20°, 30°, and 35°C were also strongly correlated ($r^2 \geq 0.98$) with HNO₂^{1.35}, with low relative standard errors (< 4%) for each coefficient (k_{PNO} , Table 4). Production rates were not correlated with NO₂⁻ concentrations alone ($r^2 < 0.10$). Temperature effects on k_{PNO} and k_{PN_2O} were well described by Arrhenius-type relationships (Figure 1b), that is, natural logarithm-transformed coefficients were strongly

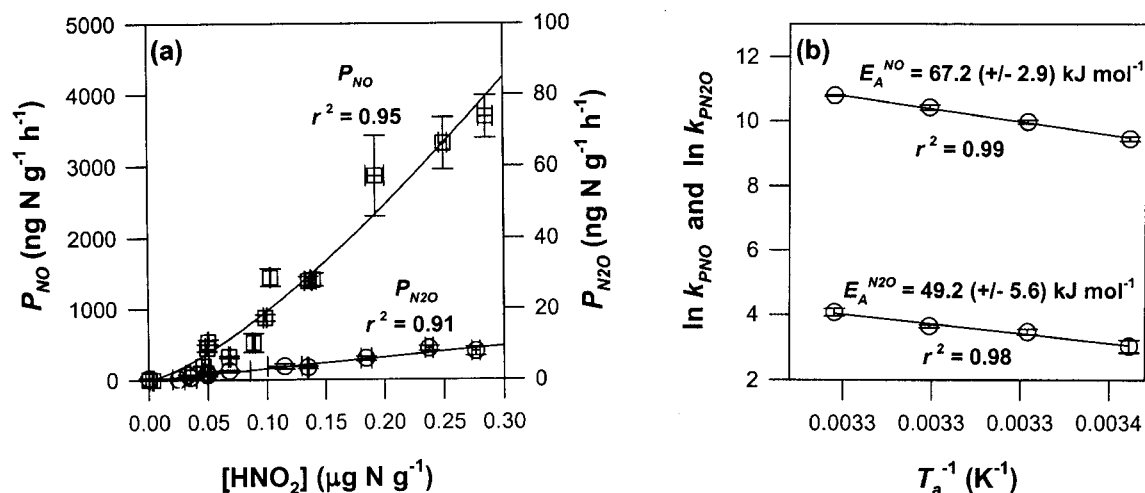


Figure 1. (a) Gross production of NO (squares) and N₂O (circles) as function of calculated soil HNO₂ in sterile soil at 25°C with standard error bars and regression lines, and (b) Arrhenius plots and estimated activation energies for k_{PNO} and k_{PN2O} .

correlated ($r^2 \geq 0.97$) with the inverse of the absolute temperatures (T_a^{-1}). Therefore activation energies were estimated based on these relationships (Figure 1b) [Pauling, 1970].

3.2. Field Soil Properties

Temporal patterns of NH₄⁺ and NO₃⁻ concentrations were typical of a nitrification-dominated system (Figures 2a and 2b). Levels of NO₂⁻ increased during the first 10 days followed by a rapid decline, although NO₂⁻ concentrations of > 0.01 μg N g⁻¹ persisted for the duration of the experiment (Figure 2c). Following AA application, pH was initially elevated above background and subsequently decreased (Figure 2d). Levels of NO₂⁻ in a sample ($\theta = 0.21$ g H₂O g⁻¹) taken on Day 12 from the 5-10 cm depth were found to decrease from 12 to < 0.1 μg N g⁻¹ soil within 48 hours after treatment with 10 Pa of C₂H₂ (data not shown). Concentrations of NO₂⁻ in an aerated untreated subsample were unchanged, indicating that the NO₂⁻ was derived primarily from nitrification in this sample.

Water contents in the upper 0-10 cm exceeded 0.25 g H₂O g⁻¹ on only one sampling day, and were significantly higher ($p < 0.01$) at the 5-10 cm than at the 0-5 cm depth (Figure 2e). Soil bulk density values (ρ) measured in intact cores were in the range of 1.30-1.35 g cm⁻³. The corresponding WFPS values

(using $\rho = 1.3$) varied over the range of < 10 to > 50% (Figure 2e). WFPS and soil temperature values were lognormally distributed within each depth and averaged over 0-10 cm. Soil temperatures were significantly higher ($p < 0.01$) at the 0-5 cm depth, consistent with expected temperature distributions for the afternoon sampling times (1300-1500 hours LT).

3.3. Field Trace Gas Fluxes

Fluxes of NO and N₂O (F_{NO} and F_{N2O}) were relatively high compared to previously published data from fertilized agricultural soils (Figures 3a and 3b), with peak fluxes of > 1000 and > 400 ng N cm⁻² h⁻¹, respectively. Temporal patterns of gas fluxes generally followed the pattern of NO₂⁻ and NH₄⁺ dynamics during the first 10-15 days, but fluxes of > 100 ng NO-N cm⁻² h⁻¹ and > 50 ng N₂O-N cm⁻² h⁻¹ persisted after > 4 weeks into the experiment. In three cases where NO fluxes of > 900 ng N cm⁻² h⁻¹ were measured, calculated theoretical errors due to O₂ oxidation of NO occurring in sampling tubes between collection and analysis were 10-15%, so these fluxes may in fact have been significantly underestimated (soil cores were not collected from beneath these chambers). Fluxes of

Table 4. Results of HNO₂-Mediated NO and N₂O Production Kinetics Experiments

Temperature, °C	NO production			N ₂ O production		
	k_{PNO}^\dagger	r^2	n	k_{PN2O}^\ddagger	r^2	n
<i>Sterile Soil</i>						
20	12.8 (0.44)	0.98	10	20.7 (2.0)	0.82	10
25	21.6 (0.65)	0.95	32	32.0 (1.4)	0.91	24
30	33.7 (1.31)	0.98	10	37.8 (0.8)	0.99	10
35	48.8 (0.58)	0.99	10	58.2 (3.3)	0.93	10
<i>Nonsterile Soil</i>						
25	9.7 (1.10)	0.68	21	-	-	-
25	7.1 (0.66) [§]	0.74 [§]	17 [§]	-	-	-

[†]Units μg NO-N μg HNO₂-N^{-1.35} h⁻¹ (standard error of coefficient in parentheses).

[‡]Units ng N₂O-N μg HNO₂-N⁻¹ h⁻¹ (standard error of coefficient in parentheses).

[§]From regression using data where HNO₂ concentrations were within the range measured in non-incubated field samples (Figure 5), $p < 0.01$ for all coefficients.

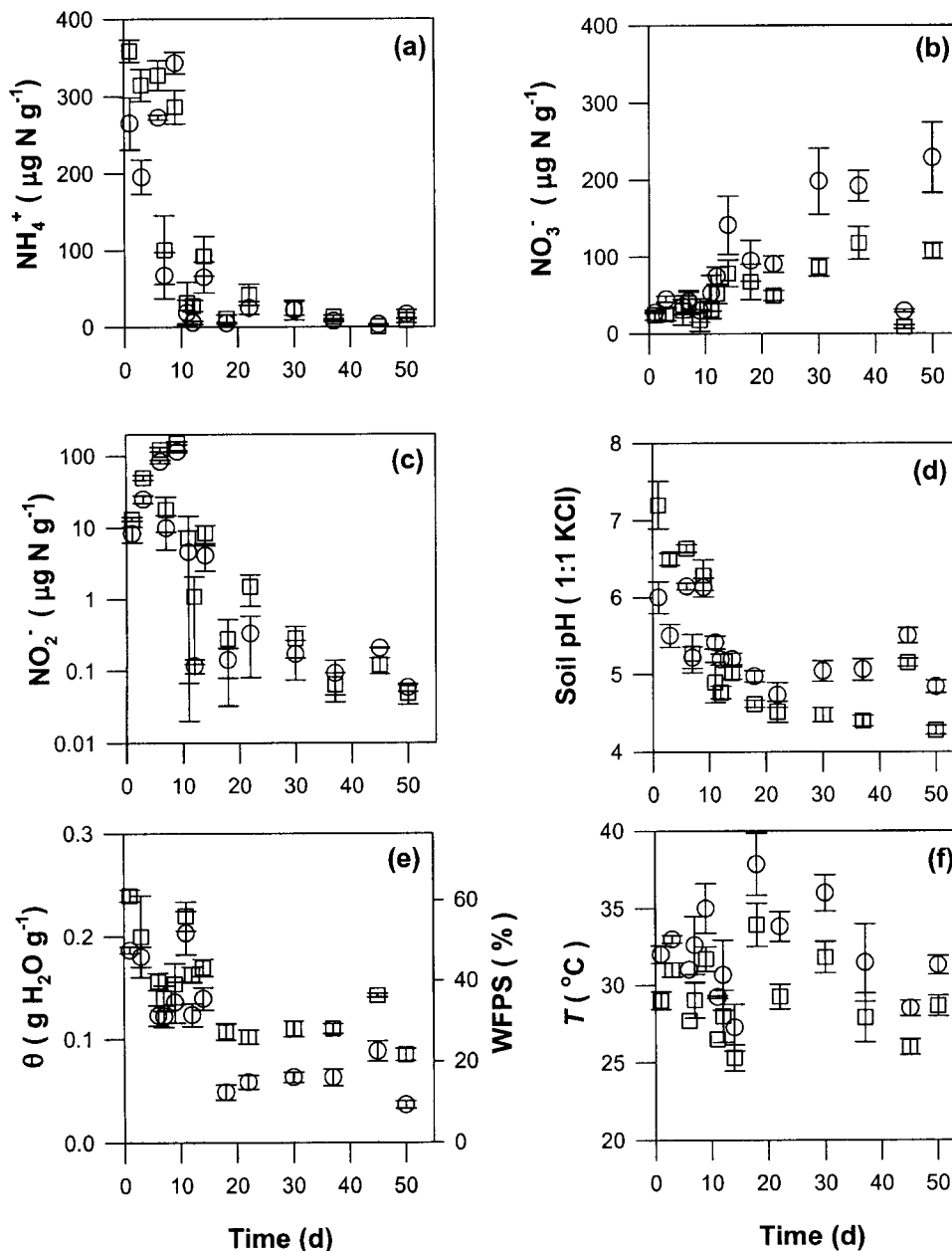


Figure 2. Mean soil concentrations of (a) NH_4^+ , (b) NO_3^- , (c) NO_2^- (log scale) and (d) soil pH, (e) water content, and (f) soil temperature, each at 0-5 (circles) and 5-10 (squares) cm with standard error bars ($n = 2-6$ per day).

CO_2 ranged from 2.3 to 40 $\mu\text{g C cm}^{-2} \text{h}^{-1}$ ($\bar{x} = 11 \pm 5.5$). Afternoon ground level O_3 concentrations ranged from 10 to 94 nL L^{-1} ($\bar{x} = 42 \pm 19.6$).

3.4. Regression Analysis of Field Data

Field F_{NO} and $F_{\text{N}_2\text{O}}$ data were normalized by log transformations, as determined by Kolmogorov-Smirnov tests. Calculated HNO_2 values were also lognormally distributed, with peak values of $> 0.20 \mu\text{g N g}^{-1}$ soil ($\bar{x} = 0.033 \pm 0.051$). Simple regression analysis yielded significant relationships ($p < 0.001$) between HNO_2 (averaged over 0-10 cm) and F_{NO} ($r^2 = 0.71$ or 0.56), and between HNO_2 and $F_{\text{N}_2\text{O}}$ ($r^2 = 0.74$ or 0.50) using untransformed or transformed variables, respectively. Simple correlations between gas fluxes and NH_4^+ ($r^2 = 0.32-0.49$) and NO_3^- ($r^2 < 0.15$) were not as strong as for HNO_2 .

Multiple regression analyses using log-transformed gas fluxes, HNO_2 , fractional WFPS (WFPS_f), and soil temperature (T) (all soil property values averaged over 0-10 cm) resulted in significant relationships ($p < 0.001$). After transformation back to original variables, these relationships take the form

$$F = [\text{HNO}_2]^\sigma T^\nu \text{WFPS}_f^\delta, \quad (4)$$

where σ , ν , and δ are the linear regression coefficients ($\delta = 0$ for F_{NO}). The models were fairly strong predictors of F_{NO} and $F_{\text{N}_2\text{O}}$ ($R^2 = 0.75-0.78$) (Table 5 and Figure 4). Residuals were normally distributed and uncorrelated with any measured variables. Similar results were obtained using untransformed variables, although for F_{NO} the model had a higher standard error of estimate (SE) and lower R^2 value (Table 5). Although

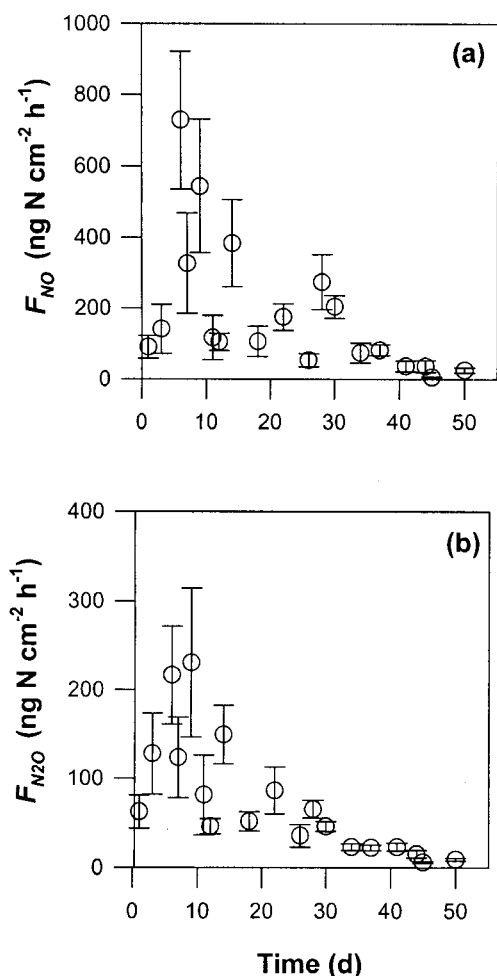


Figure 3. Mean surface fluxes of (a) NO and (b) N₂O with standard error bars ($n = 4-9$ per day).

mean NO and N₂O fluxes predicted by the models were similar to actual values (94 and 90%, respectively), SE values were relatively high indicating that the models did not account for important controlling factors. Unexplained variability may be due to factors related to gas transport in porous media and variations in NO and N₂O consumption processes, which are not accounted for in these models. The F_{CO_2} data did not help to explain variability in F_{NO} or F_{N_2O} . Fluxes of CO₂ were correlated with θ and T , but these factors did not explain much of the variability in F_{CO_2} ($R^2 = 0.12$).

3.5. HNO₂-Mediated NO Production Kinetics in Non-Sterile Soils

Gross NO production rates (P_{NO}) and corresponding HNO₂ concentrations in nonsterile soils collected from the field in 1998 and incubated aerobically at 25°C are shown in Figure 5. Based on results of the sterile soil kinetic experiments, regression analysis of P_{NO} versus HNO₂^{1,35} was performed. Two separate regression analyses were performed: (1) using all data ($n = 21$), and (2) using only data ($n = 17$) where HNO₂ concentrations were $\leq 0.22 \mu\text{g N g}^{-1}$. The latter regression analysis included only data for which the HNO₂ levels were within the range measured in field samples ($n = 122$) which were not incubated in the laboratory prior to analysis and for which corresponding gas flux measurements were available. In either case (i.e., $n = 17$ or $n = 21$), resulting values of the rate coef-

ficient (k_{PNO}) were less than in sterile soil with more unexplained variability ($r^2 = 0.68-0.70$, Table 4).

3.6. Application of Modified Galbally and Johansson Model

Measured F_{NO} values were compared to predictions of a modified model based on that of Galbally and Johansson [1989], which relates laboratory measurements of P_{NO} and k_c to field NO flux using the exact solution to a steady-state one-dimensional reaction-diffusion equation:

$$F_{NO} = \left(\frac{P_{NO}}{k_c} - [NO]_o \right) \sqrt{\tau D_o k_c \rho}, \quad (5)$$

where D_o is the gas diffusion coefficient for NO in air (cm² gas h⁻¹), τ is a soil gas diffusion coefficient reduction factor (cm gas cm⁻¹ soil), and $[NO]_o$ is the ambient NO concentration (ng N cm⁻³ gas). The Chapman-Enskog model [Bird *et al.*, 1960] was used to calculate D_o as a function of temperature (0-10 cm). The soil gas tortuosity model of Moldrup *et al.* [1997]

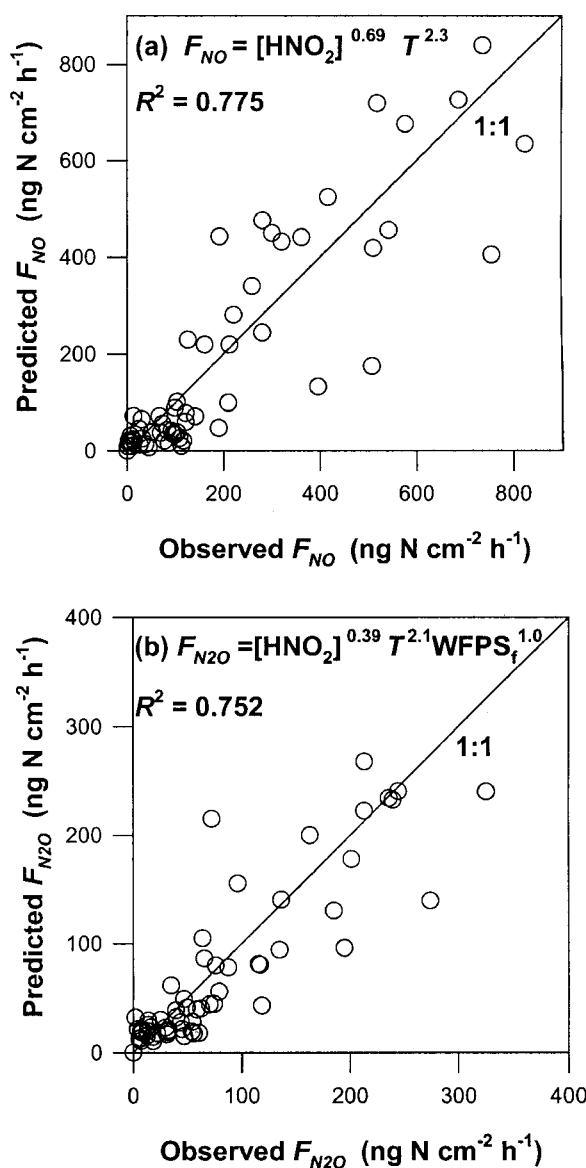


Figure 4. Multiple regression model results for (a) F_{NO} and (b) F_{N_2O} , using (4) and Table 5.

Table 5. Multiple Regression Results for F_{NO} and F_{N_2O}

Predicted Variable	Regression coefficients [†]				SE [‡]	R ²
	σ	v	δ			
F_{NO}	0.69	2.3	--		103(115)	0.78 (0.72)
F_{N_2O}	0.39	2.1	1.0		39 (39)	0.75 (0.76)

[†]Per equation (4) relating HNO₂, temperature, and WFPS to F_{NO} and F_{N_2O} ; WFPS was not a significant factor ($p > 0.19$) for F_{NO} ; all other coefficients were significant ($p < 0.001$).

[‡]Standard error of estimate; units ng N cm⁻² h⁻¹ (SE and R² values in parentheses are for models using untransformed variables).

was used to estimate τ as a function of θ and ρ , and a value of 0.00053 ng N cm⁻³ was used for [NO]₀ [Galbally and Johansson, 1989].

The laboratory kinetic data allowed for expression of P_{NO} as a function of HNO₂ and absolute soil temperature (T_a) (each averaged over 0-10 cm) incorporating the Arrhenius relation:

$$P_{NO} = [HNO_2]^{1.35} \exp\left(A_o - \frac{E_A^{NO}}{RT_a}\right) \quad (6)$$

The k_{PNO} values obtained from regression of nonsterile P_{NO} versus HNO₂^{1.35} at 25°C were used to determine A_o using (6) with $T_a = 298$ K and $E_A^{NO} = 67.2$ kJ mol⁻¹. Values for A_o of 36.3 and 36.0 were obtained using either $n = 21$ or $n = 17$, respectively (Figure 5 and Table 4). Values of P_{NO} calculated using (6) were then used to predict F_{NO} using (5), assuming a temperature-dependency factor (Q_{10}) of 2.0 applied to the mean k_c value (30 cm³ gas g⁻¹ soil h⁻¹) (model output was not very sensitive to varying Q_{10} over the range of 1.5-3.0). Accuracy of model performance was evaluated using the root-mean-square error (RMSE) index and the degree of model overprediction or underprediction was evaluated using the bias (b) index [Moldrup et al., 1997]:

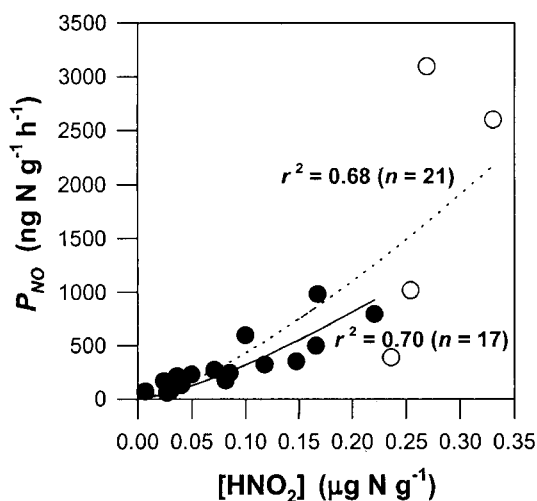


Figure 5. Gross NO production (P_{NO}) and HNO₂ concentrations in nonsterile aerobically incubated soil at 25°C and regression lines for P_{NO} versus HNO₂^{1.35} for $n = 21$ (dotted line) or $n = 17$ (solid line) samples. Open symbols indicate data points ($n = 4$) where HNO₂ concentrations were above the range measured in nonincubated field samples (these points were excluded from regression with $n = 17$).

$$RMSE = \sqrt{\frac{1}{n} \sum_{i=1}^n d_i^2} \quad (7)$$

$$b = \frac{1}{n} \sum_{i=1}^n d_i \quad (8)$$

where d_i is the predicted value minus the observed value for observation i , and n is total number of observations. Predicted versus observed F_{NO} values are shown in Figure 6 using $A_o = 36.0$. The model tended to underestimate fluxes under lower flux conditions (i.e., $b < 0$ for $F_{NO} < 250$ ng N cm⁻² h⁻¹, $n = 44$) and overestimate under higher flux conditions ($b > 0$ for $F_{NO} > 250$ ng N cm⁻² h⁻¹, $n = 17$). Using an A_o value of 36.3 produced the same trends, but with less accuracy (overall RMSE = 370) and greater overestimation under high flux conditions ($b = 430$ for $F_{NO} > 250$ ng N cm⁻² h⁻¹).

3.7. NO-Mediated N₂O Production

In C₂H₂-treated (10 Pa) soil at WFPS values of 20, 40, and 60%, mean N₂O production increased with mean NO concentrations during the incubation period (Figure 7a and Table 6). At each level of WFPS, the data were analyzed with the assumption of first-order reaction kinetics with respect to NO concentration, that is,

$$P_{N_2O}^d = P_{N_2O}^a + k_t [NO] \quad (9)$$

where $P_{N_2O}^d$ = net denitrification-derived N₂O production rate (ng N g⁻¹ soil h⁻¹), $P_{N_2O}^a$ = denitrification-derived N₂O production rate in absence of NO (ng N g⁻¹ soil h⁻¹), k_t = first-order NO to N₂O transformation rate coefficient (ng N₂O-N cm³ gas ng⁻¹ NO-N g⁻¹ soil h⁻¹), and [NO] = NO concentration (ng N cm³ gas). This formulation considers the gas phase NO concentration as the driving factor promoting N₂O production above a baseline level ($P_{N_2O}^a$). Values of $P_{N_2O}^a$ and k_t obtained

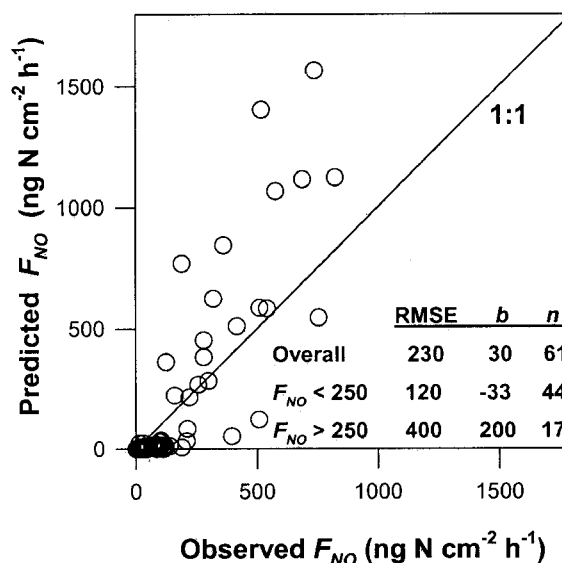


Figure 6. Observed F_{NO} versus predictions of modified Galbally and Johansson [1989] model, (5) and (6), with $A_o = 36.0$. RMSE, root-mean-square error (equation (7)), b , bias (equation (8)).

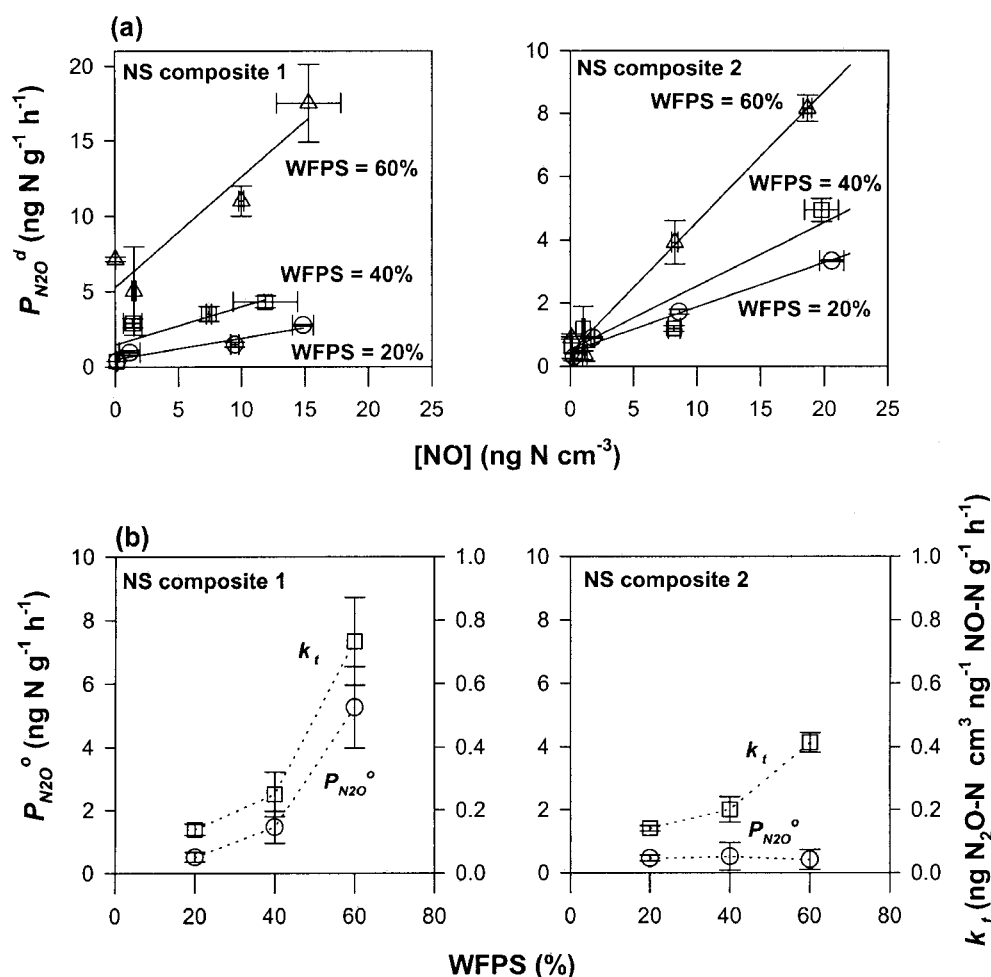


Figure 7. (a) Effect of gas phase NO on the denitrification-derived N₂O production rate ($P_{N_2O}^d$) at varying WFPS with regression lines, and (b) effect of WFPS on the denitrification-derived N₂O production rate in absence of NO ($P_{N_2O}^o$) and the first-order NO to N₂O transformation coefficient (k_t) (equation (9)).

by regression of measured $P_{N_2O}^d$ versus [NO] increased with increasing WFPS (Figure 7b and Table 6). Measurements of total NO transformation rate coefficients (k_c , equation (1)) were used to estimate the fraction of total transformed NO which was converted to N₂O (f_{N_2O} , ng N₂O-N ng⁻¹ NO-N):

$$f_{N_2O} = \frac{k_t}{k_c} \quad (10)$$

Measured k_c values were in the range of 13–44 cm³ gas g⁻¹ soil h⁻¹, yielding f_{N_2O} values of 0.003–0.05. Thus, while production of N₂O was enhanced by NO transformation, most of the transformed NO (i.e., ≥ 95%) did not end up as N₂O.

4. Discussion

4.1. HNO₂-Mediated Kinetics

Our results show that the magnitude of abiotic NO production per unit of HNO₂ is 5–10 times greater than previously observed and is higher than would be predicted based on correlations between k_{PNO} and soil organic matter (SOM) content [Venterea and Rolston, 2000]. Also, the nonlinear dependency of NO production on HNO₂ (i.e., apparent reaction order of 1.35) which was consistently observed at all tempera-

tures differs from previous data [Venterea and Rolston, 2000] where a linear dependency was found. This behavior and the higher rates of abiotic NO production in this soil may have been related to specific SOM functional constituents which can react with HNO₂ to produce NO [Stevenson, 1994] and/or to reactions of HNO₂ with soil mineral constituents [Nelson, 1982]. The observed activation energy for abiotic NO production ($E_A^{NO} = 67$ kJ mol⁻¹) is similar to values reported from a variety of field sites, which generally have ranged from 44 to 108 kJ mol⁻¹ [Slemr and Seiler, 1984; Johansson and Granat, 1984; Williams *et al.*, 1987; Shepherd *et al.*, 1991; Skiba *et al.*, 1992]. Previously reported values have been calculated from relationships between soil temperatures and net field emissions, which can be influenced by several microbial, physical, and chemical processes, each of which may be temperature sensitive to varying degrees. Values reported here are therefore mechanism-specific to a greater extent, because they apply to rate coefficients exclusive to abiotic HNO₂-mediated production.

The reduced rate of NO production per unit HNO₂ in the nonsterile compared to sterile soil at 25°C (Table 4) is consistent with previous results where this trend was attributed to biological competition for available substrate (NO₂⁻) in incubated nonsterile soil [Venterea and Rolston, 2000]. The present data also indicate a higher degree of variability, which

Table 6. Results of NO-Mediated N₂O Production Experiment

WFPS, %	k_t^\dagger	$P_{N_2O}^\ddagger$	$r^{2\S}$	n
<i>Nonsterile Composite 1</i>				
20	0.14 (0.02)	0.51 (0.16)	0.91	8
40	0.25 (0.07)	1.46 (0.51)	0.68	8
60	0.73 (0.14)	5.26 (1.28)	0.82	8
<i>Nonsterile Composite 2</i>				
20	0.14 (0.01)	0.46 (0.10)	0.98	8
40	0.20 (0.04)	0.52 (0.44) [¶]	0.80	8
60	0.41 (0.03)	0.42 (0.32) [¶]	0.97	8

[†]First-order NO to N₂O transformation rate coefficient; units ng N₂O-N cm³ ng⁻¹ NO-N g⁻¹ h⁻¹ (standard error of coefficient in parentheses), $p < 0.03$.

[‡]Denitrification-derived N₂O production rate in absence of NO; units ng N₂O-N g⁻¹ h⁻¹ (standard error of coefficient in parentheses), $p < 0.01$ except where indicated.

[§]For regression of mean N₂O production rate versus mean NO concentration (Figure 7a), equation (9).

[¶] P_{N_2O} values not significantly different than 0 ($p > 0.20$).

is not accounted for solely by HNO₂ concentrations in the nonsterile compared to sterile soil data (Figures 1a and 5 and Table 4). This may have been due to variations in the extent of competing biological activity in nonsterile samples, and/or to differences in SOM levels which were shown in the previous study to be well correlated with k_{PNO} values. The processes of air drying and sieving the sterilized soil may also have modified the reactive soil constituents compared to nonsterile samples which were not sieved. Further studies are required to examine other factors which may influence these rate coefficients for NO production. The k_{PNO} value measured in λ -irradiated soil at 25°C is in the same range of values obtained in a previous study [Venterea and Rolston, 2000]. Earlier studies have shown that N₂O can be produced from reactions of HNO₂ with SOM constituents [Stevenson, 1994].

4.2. Field NO₂⁻ Accumulation and Trace Gas Emissions

Accumulation of > 100 $\mu\text{g NO}_2^- \text{-N g}^{-1}$ has been observed following AA application and is often attributed to the toxicity of free NH₃ toward *Nitrobacter* populations [Chalk et al., 1975; Van Cleemput and Samater, 1996]. Alkaline conditions promote the dissociation of NH₄⁺ to NH₃ ($pK_a = 9.3$) [Smith et al., 1997]. In this study, NO₂⁻ concentrations of 0.2–4.5 $\mu\text{g N g}^{-1}$ persisted even after 20 days when pH and NH₄⁺ levels had declined to < 5.5 and < 100 $\mu\text{g N g}^{-1}$, respectively. This suggests that NO₂⁻ accumulation may have been also influenced by other factors, such as HNO₂, which itself has been shown to inhibit *Nitrobacter* activity in liquid culture studies [Hunik et al., 1993]. Also, after 18 days, calculated liquid phase concentrations of NO₃⁻ were 240 (+197) and 60 (+36) mM over the 0–5 and 5–10 cm depths, respectively. Nitrate-N concentrations of ≥ 40 mM have been found to inhibit *Nitrobacter* activity, with a more pronounced effect at lower pH [Hunik et al., 1993].

The conditions of low pH and high NH₄⁺ and NO₂⁻ levels, together with the apparently unique kinetic properties (i.e., high k_{PNO}), combined to generate some of the highest N trace gas fluxes reported from agricultural systems [Eichner, 1990; Veldkamp and Keller, 1997a]. Overall mean NO fluxes (190 \pm 215 ng N cm⁻² h⁻¹) are comparable to mean midday fluxes of 300–550 ng N cm⁻² h⁻¹ reported by Matson et al. [1998] from intensively fertilized wheat fields in Mexico. Peak NO fluxes

(> 1000 ng N cm⁻² h⁻¹) are comparable to maximum NO fluxes (~ 800 ng N cm⁻² h⁻¹) measured in urea-fertilized fields in Spain [Slemr and Seiler, 1984]. Peak N₂O fluxes similar to those observed here (300–400 ng N cm⁻² h⁻¹) have been measured in AA-fertilized corn and soybean fields in the United States [Bremner et al., 1981; Thornton et al., 1996].

4.3. Mechanistic Modeling

It is likely that several assumptions of the Galbally and Johansson [1989] model were violated under the present field conditions. That is, the model considers steady-state conditions, one-dimensional vertical diffusion and also assumes that physical properties and chemical and microbial processes are uniform throughout the soil profile. For example, the localized distribution of N resulting from the fertilizer application method produced significant gradients in inorganic N concentrations and soil pH over a few centimeters in both the horizontal and vertical directions (data not shown). This would be likely to cause significant gradients in N oxide gas concentrations in two or three dimensions. Thus the vertical transport within any soil profile and the net flux from any section of the soil-atmosphere interface are likely to be influenced by dynamics in adjacent profiles. Lateral gaseous diffusion away from “hot spots” would tend to reduce emissions directly above these zones while increasing emissions from adjacent areas. This description is in fact consistent with the pattern of deviation observed between measured NO fluxes and those predicted by the model. That is, the model generally over-predicted F_{NO} from higher-flux locations while underpredicting lower-flux locations (Figure 6). The modified model predictions are also highly dependent on the A_n value used in (6) and therefore also on regression of the nonsterile kinetic data (i.e., P_{NO} versus HNO₂, Figure 5). An additional assumption of the modified model was that the A_n value was constant in all samples, which is equivalent to assuming that the k_{PNO} value at any temperature was constant. However, unexplained variability in the relationship between P_{NO} and HNO₂ ($r^2 \sim 0.7$) suggests that this assumption may have also been responsible for errors in model predictions. Based on previous results indicating a strong positive relationship between k_{PNO} values and SOM levels in three different soils [Venterea and Rolston, 2000], it is possible that differences in SOM between samples were responsible for some of the observed variability. Disturbance of the in situ soil structure and aeration status prior to laboratory analysis may also have altered the processes affecting NO production kinetics. Thus a more complete mechanistic description with less restrictive assumptions than in the Galbally and Johansson [1989] model may be required to more accurately predict NO fluxes under the present or similar field conditions, and further studies are required to examine additional factors influencing NO production kinetics.

4.4 NO-Mediated N₂O Production

The standard error of the coefficients (Table 6) range from 7 to 28% of the estimated k_t values, suggesting that the assumption of NO-dependent first-order kinetics is only partly adequate in describing the kinetics (Figure 7). Unexplained variability in N₂O production can be attributed to variations in other factors which are known to influence reductive microbial processes, such as dissolved organic carbon levels and small-scale soil aggregate structure which can affect microsite anoxia. These factors may have varied between the subsamples even though the composite samples were well mixed prior to testing.

Nonetheless, the data give a strong indication that NO reduction to N₂O is a potentially important source of N₂O even under bulk aerobic and relatively dry soil conditions and provide at least a preliminary kinetic description. This result is consistent with studies using liquid cultures of denitrifying soil bacteria with nitric oxide reductase enzyme systems [Schafer and Conrad, 1993]. Direct microbial reduction of NO to N₂O may not have been the only process which was enhanced at higher NO concentrations. All soils initially had nondetectable levels of NO₂⁻, but increases of 0.4–1 μg N g⁻¹ were observed after 1–2 hours in high-[NO] treatments, possibly due to microbial and/or chemical oxidation of NO. Production of N₂O due to abiotic reduction of generated HNO₂ was calculated (equation (3)) to be 0.3–0.9 ng N₂O-N g⁻¹ soil h⁻¹ in the high-[NO] treatments. Increases in P'_{N₂O} at increasing WFPS in NS composite 1 indicate that the dissimilatory NO₃⁻ reduction sequence, that is, NO₃⁻ → NO₂⁻ → NO → N₂O, was occurring in the absence of added NO. This process was demonstrated to be important even under similar bulk aerobic conditions in a recent study using three agricultural soils amended with ¹⁵NO₃⁻ [Venterea and Rolston, 2000]. The low to nonsignificant P'_{N₂O} values observed in NS composite 2 (Table 6) likely resulted from the longer sample storage period under air-dried conditions, which could have affected the viability of facultative anaerobic microbes mediating NO₃⁻ reduction.

An important implication of the present laboratory and field data is that given high rates of NO production, the production of N₂O resulting from microbial transformations of NO can be significant even under relatively dry and aerobic soil conditions. The generally high rate of field N₂O emissions (Figure 3b) which occurred despite the relatively low WFPS conditions in the upper 10 cm (Figure 2e) suggests that reduction of abiotically produced NO may have been more important as a source of N₂O than dissimilatory NO₃⁻ reduction under the given field conditions. It is possible that dissimilatory NO₃⁻ reduction occurring at depths > 10 cm, under wetter and less oxic conditions, may have significantly contributed to field N₂O emissions. The lack of data from these depths therefore limits our conclusions regarding the relative importance of NO-mediated versus denitrification-mediated N₂O emissions at this site.

4.5. Concluding Remarks

The acidification of agricultural soils as a result of repeated application of N fertilizers can only be expected to increase in significance as world-wide fertilizer use increases, unless specific management practices are undertaken. In light of this fact, the present data, and existing gaps in accounting for global sources of NO and N₂O, further investigation of the role of biotic/abiotic mechanisms as promoted by NO₂⁻ accumulation and acidity in agricultural soil is required. Studies across a range of ecosystems are needed to further elucidate and delineate the importance of HNO₂-driven soil-atmosphere exchange of N trace gases. Models of N trace gas emissions at varying spatial and temporal scales also need to consider the factors affecting these biotic/abiotic mechanisms.

Notation

A_0	exponential factor in Arrhenius relation.
b	bias, ng NO-N cm ⁻² h ⁻¹ .
D_0	gas diffusion coefficient for NO in air, cm ² gas h ⁻¹ .
E_A	activation energy, kJ mol ⁻¹ .

f_{N_2O}	fraction of total transformed NO produced as N ₂ O, ng N ₂ O-N ng ⁻¹ NO-N.
F_{CO_2}	soil-atmosphere CO ₂ flux, μg C cm ⁻² h ⁻¹ .
F_{NO}	soil-atmosphere NO flux, ng N cm ⁻² h ⁻¹ .
F_{N_2O}	soil-atmosphere N ₂ O flux, ng N cm ⁻² h ⁻¹ .
[HNO ₂]	calculated nitrous acid concentration, μg HNO ₂ -N g ⁻¹ soil.
k_c	first-order NO consumption rate coefficient, cm ³ gas g ⁻¹ soil h ⁻¹ .
k_{PNO}	NO production rate coefficient, ng NO-N μg HNO ₂ -N ^{-α} h ⁻¹ .
k_{PN_2O}	N ₂ O production rate coefficient, ng N ₂ O-N μg HNO ₂ -N ^{-β} h ⁻¹ .
k_t	NO to N ₂ O transformation rate coefficient, ng N ₂ O-N cm ³ gas ng ⁻¹ NO-Ng ⁻¹ h ⁻¹ .
[NO]	gas phase NO concentration, ng N cm ⁻³ gas.
[NO] _e	gas phase NO concentration in effluent of well-mixed reaction chamber, ng N cm ⁻³ .
[NO] _o	ambient gas phase NO concentration, ng N cm ⁻³ .
P_{net}	net NO production rate, ng N g ⁻¹ soil h ⁻¹ .
P_{NO}	gross NO production rate, ng N g ⁻¹ soil h ⁻¹ .
P_{N_2O}	gross overall N ₂ O production rate, ng N g ⁻¹ soil h ⁻¹ .
P'_{N_2O}	net denitrification-derived N ₂ O production rate, ng N g ⁻¹ soil h ⁻¹ .
P''_{N_2O}	denitrification-derived N ₂ O production rate in absence of NO, ng N g ⁻¹ soil h ⁻¹ .
R	universal gas constant, 8.31 × 10 ⁻³ kJ K ⁻¹ mol ⁻¹ .
R^2	coefficient of multiple regression.
r^2	coefficient of simple regression.
RMSE	root-mean-square error of estimate for mechanistic model, ng NO-N cm ⁻² h ⁻¹ .
SE	standard error of estimate for regression models, ng N cm ⁻² h ⁻¹ .
T	soil temperature, °C.
T_a	absolute soil temperature, K.
WFPS	water-filled pore space, percent basis, cm ³ H ₂ O cm ⁻³ pore space × 100%.
WFPS _f	water-filled pore space, fractional basis, cm ³ H ₂ O cm ⁻³ pore space.
α	apparent reaction order for HNO ₂ -derived NO production.
β	apparent reaction order for HNO ₂ -derived N ₂ O production.
θ	gravimetric soil water content, g H ₂ O g ⁻¹ soil.
ρ	soil dry bulk density, g soil cm ⁻³ dry soil.
ρ_w	liquid water density, g H ₂ O cm ⁻³ H ₂ O.
σ, ν, δ	multiple regression coefficients.
τ	soil gas diffusion coefficient reduction factor, cm gas cm ⁻¹ soil.

Acknowledgments. The authors gratefully acknowledge Y. O'Quinn, M. Quok, and R.G. Cabral for assistance with the field and laboratory work, D.T. Louie for technical assistance, C. Anastasio for helpful discussion, and two anonymous reviewers for their helpful criticisms. This work was supported in part by the Kearney Foundation of Soil Science and in part by the U.S. EPA (R819658 and 825433) Center for Ecological Health Research at U.C. Davis, although it may not necessarily reflect the views of the EPA, and no official endorsement should be inferred.

References

- Anderson, I., and J. Levine, Simultaneous field measurements of biogenic emissions of nitric oxide and nitrous oxide, *J. Geophys. Res.*, 92, 965–976, 1987.
- Atkinson, R., D. Baulch, R. Cox, J. R. Hampson, J. Kerr, M.

- Rossi, and J. Troe, Evaluated kinetic and photochemical data for atmospheric chemistry: Supplement VI, IUPAC subcommittee on gas kinetic data evaluation for atmospheric chemistry, *J. Phys. Chem. Ref. Data*, 26, 1329-1499, 1997.
- Bird, R., W. Stewart, and E. Lightfoot, *Transport Phenomena*, pp. 510-513, John Wiley, New York, 1960.
- Blackmer, A., and M. Cerrato, Soil properties affecting formation of nitric oxide by chemical reactions of nitrite, *Soil Sci. Soc. Am. J.*, 50, 1215-1218, 1986.
- Bouman, O., D. Curtin, C. Campbell, V. Biederbeck, and H. Ukrainetz, Soil acidification from long-term use of anhydrous ammonia and urea, *Soil Sci. Soc. Am. J.*, 59, 1488-1494, 1995.
- Bremner, J., Sources of nitrous oxide in soils, *Nutrient Cycling Agroecosyst.*, 49, 7-16, 1997.
- Bremner, J., G. Breitenbeck, and A. Blackmer, Effect of anhydrous ammonia fertilization on emissions of nitrous oxide from soils, *J. Environ. Qual.*, 10, 77-80, 1981.
- California Department of Food and Agriculture, Fertilizing Materials Tonnage Report, Sacramento, January-June, 1998.
- Chalk, P., D. Keeney, and L. Walsh, Crop recovery and nitrification of fall and spring applied anhydrous ammonia, *Agron. J.*, 67, 33-41, 1975.
- Crutzen, P., The role of NO and NO₂ in the chemistry of the troposphere and stratosphere, *Ann. Rev. Earth Planet. Sci.*, 7, 443-472, 1979.
- Crutzen, P., Atmospheric chemical processes of the oxides of nitrogen, including nitrous oxide, in *Denitrification, Nitrification and Atmospheric N₂O*, edited by C. Delwiche, pp. 17-44, John Wiley, New York, 1981.
- Davidson, E. A., Fluxes of nitrous oxide and nitric oxide from terrestrial ecosystems, in *Microbial Production and Consumption of Greenhouse Gases: Methane, Nitrogen Oxide, and Halomethanes*, edited by J. E. Rogers and W. B. Whitman, pp. 219-235, Am. Soc. for Microbiol., Washington, D. C., 1991.
- Davidson, E. A., and W. Kinglerlee, A global inventory of nitric oxide emissions from soils, *Nutrient Cycling Agroecosyst.*, 48, 37-50, 1997.
- Davidson, E. A., W. Swank, and T. Perry, Distinguishing between nitrification and denitrification as sources of gaseous nitrogen production in soil, *Appl. Environ. Microbiol.*, 52(6), 1280-1286, 1986.
- Davidson, E. A., P. Vitousek, P. Matson, R. Riley, G. Garcia-Mendez, and J. Maass, Soil emissions of nitric oxide in a seasonally dry tropical forest of Mexico, *J. Geophys. Res.*, 96, 15,439-15,445, 1991.
- Delucchi, M., J. Murphy, J. Kim, and D. McCubbin, The cost of crop damage caused by ozone air pollution from motor vehicles, in *The Annualized Social Cost of Motor-Vehicle Use in the United States, Rep. UCD-ITS-RR-96-3 (12)*, Inst. of Transp. Stud., Univ. of Calif., Davis, 1996.
- Eichner, M., Nitrous oxide emissions from fertilized soils: Summary of available data, *J. Environ. Qual.*, 19, 272-280, 1990.
- Firestone, M., and E. Davidson, Microbiological basis of NO and N₂O production and consumption in soil, in *Exchange of Trace Gases Between Terrestrial Ecosystems and the Atmosphere*, edited by M. Andreae and D. Schimel, pp. 7-21, John Wiley, New York, 1989.
- Frederick, L., and F. Broadbent, Biological interactions, in *Agricultural Anhydrous Ammonia Technology and Use*, edited by M. H. McVickar et al., pp.198-212, Agric. Ammonia Inst., Memphis, Tenn., 1965.
- Galbally, I., and C. Johansson, A model relating laboratory measurements of rates of nitric oxide production and field measurements of nitric oxide emission from soils, *J. Geophys. Res.*, 94, 6473-6480, 1989.
- Heck, W., Assessment of crop losses from air pollutants in the United States, in *Air Pollution's Toll on Forests and Crops*, edited by J. MacKenzie and M. El-Ashry, pp. 235-313, Yale Univ. Press, New Haven, Conn., 1989.
- Holopainen, J., Ozone levels and plant growth, *Trends Plant Sci.*, 1, 368-369, 1996.
- Hunik, J., H. Meijer, and J. Tramper, Kinetics of *Nitrobacter agilis* at extreme substrate, product and salt concentrations, *Appl. Microbiol. Biotechnol.*, 40, 442-448, 1993.
- Hutchinson, G., and E. Brams, NO versus N₂O emissions from an NH₃-amended Bermuda grass pasture, *J. Geophys. Res.*, 97, 9889-9896, 1992.
- Hutchinson, G. L., and A. R. Mosier, Improved soil cover method for field measurement of nitrous oxide fluxes, *Soil Sci. Soc. Am. J.*, 45, 311-316, 1981.
- Johansson, C., and L. Granat, Emission of nitric oxide from arable land, *Tellus*, 36B, 25-37, 1984.
- Keeney, D., and D. Nelson, Nitrogen-inorganic forms, in *Methods of Soil Analysis, Part 2, Chemical and Microbiological Properties*, edited by A. Page, R. Miller, and D. Keeney, pp. 643-698, Am. Soc. of Agron., Madison, Wisc., 1982.
- Matson, P. A., NO₂ emission from soils and its consequences for the atmosphere and biosphere: Critical gaps and research directions for the future, *Nutrient Cycling Agroecosyst.*, 48, 1-6, 1997.
- Matson, P. A., R. Naylor, and I. Ortiz-Monasterio, Integration of environmental, agronomic, and economic aspects of fertilizer management, *Science*, 280, 112-115, 1998.
- McKenney, D., C. Lazar, and W. Findlay, Kinetics of the nitrite to nitric oxide reaction in peat, *Soil Sci. Soc. Am. J.*, 54, 106-112, 1990.
- Moldrup, P., T. Olesen, D. Rolston, and T. Yamaguchi, Modeling diffusion and reaction in soils, VII, Predicting gas and ion diffusivity in undisturbed and sieved soils, *Soil Sci.*, 162, 632-640, 1997.
- Mosier, A., J. Duxbury, J. Freney, O. Heinemeyer, and K. Minami, Nitrous oxide emissions from agricultural fields: Assessment, measurement and mitigation, *Plant Soil*, 181, 95-108, 1996.
- Nelson, D., Gaseous losses of nitrogen other than through denitrification, in *Nitrogen in Agricultural Soils*, edited by F. Stevenson, pp. 327-364, Am. Soc. of Agron, Madison, Wisc., 1982.
- Pauling, L., *General Chemistry*, pp. 286, 565, Dover, Mineola, N. Y., 1970.
- Prinn, R., D. Cunnold, R. Rasmussen, P. Simmonds, F. Alyea, A. Crawford, P. Fraser, and R. Rosen, Atmospheric emissions and trends of nitrous oxide deduced from 10 years of ALE-GAGE data, *J. Geophys. Res.*, 95, 18,369-18,385, 1990.
- Remde, A., F. Slemr, and R. Conrad, Microbial production and uptake of nitric oxide in soil, *FEMS Microbiol. Ecol.*, 62, 221-230, 1989.
- Reuss, J., and R. Smith, Chemical reactions of nitrites in acid soils, *Soil Sci. Soc. Am. Proc.*, 29, 267-270, 1965.
- Rodhe, H., A comparison of the contribution of various gases to the greenhouse effect, *Science*, 248, 1217-1219, 1990.
- Saylor, R., W. Chameides, and E. Cowling, Implications of the new ozone National Ambient Air Quality Standards for compliance in rural areas, *J. Geophys. Res.*, 103, 31,137-31,141, 1998.
- Schafer, F., and R. Conrad, Metabolism of nitric oxide by *Pseudomonas stutzeri* in culture and in soil, *FEMS Microbiol. Ecol.*, 102, 119-127, 1993.
- Serca, D., R. Delmas, C. Jambert, and L. Labroque, Emissions of nitrogen oxides from equatorial rain forest in central Africa: Origin and regulation of NO emissions from soils, *Tellus*, 46B, 243-254, 1994.
- Shepherd, M., S. Barzetti, and D. Hastie, The production of atmospheric NO, and N₂O from a fertilized agricultural soil, *Atmos. Environ.*, 25A, 1961-1969, 1991.
- Skiba, U., K. Hargreaves, D. Fowler, and K. Smith, Fluxes of nitric and nitrous oxides from agricultural soils in a cool temperate climate, *Atmos. Environ.*, 26A, 2477-2488, 1992.
- Slemr, F., and W. Seiler, Field measurements of NO and NO₂ emissions from fertilized and unfertilized soils, *J. Atmos. Chem.*, 2, 1-24, 1984.
- Smith, C., and P. Chalk, Gaseous nitrogen evolution during nitrification of ammonia fertilizer and nitrite transformations in soils, *Soil Sci. Soc. Am. J.*, 44, 277-282, 1980.
- Smith, R., R. Doyle, L. Burns, and R. Stevens, A model for nitrite accumulation in soils, *Soil Biol. Biochem.*, 29, 1241-1247, 1997.
- Stehouwer, R., and J. Johnson, Urea and anhydrous ammonia management for conventional tillage corn production, *J. Prod. Agric.*, 3, 507-513, 1990.
- Stevenson, F., *Humus Chemistry: Genesis, Composition, Reactions*, pp. 106-112, John Wiley, New York, 1994.
- Stohl, A., E. Williams, G. Wotawa, and H. Kromp-Kolb, A European inventory of soil nitric oxide emissions and the effect of these emissions on the photochemical formation of ozone, *Atmos. Environ.*, 30, 3741-3755, 1996.
- Strong, W., and J. Cooper, Application of anhydrous ammonia or

- urea during the fallow period for winter cereals on the Darling Downs, Queensland, I, Effect of time of application on soil mineral N at sowing, *Aust. J. Soil Sci.*, *30*, 695-709, 1992.
- Thornton, F., B. Bock, and D. Tyler, Soil emissions of nitric oxide and nitrous oxide from injected anhydrous ammonium and urea, *J. Environ. Qual.*, *25*, 1378-1384, 1996.
- Van Cleemput, O., and A. Samater, Nitrite in soils: Accumulation and role in the formation of gaseous N compounds, *Fert. Res.*, *45*, 81-89, 1996.
- Veldkamp, E., and M. Keller, Fertilizer-induced nitric oxide emissions from agricultural soils, *Nutrient Cycling Agroecosyst.*, *48*, 69-77, 1997a.
- Veldkamp, E., and M. Keller, Nitrogen oxide emissions from a banana plantation in the humid tropics, *J. Geophys. Res.*, *102*, 15,889-15,898, 1997b.
- Venterea, R., and D. Rolston, Mechanisms and kinetics of nitric and nitrous oxide production during nitrification in agricultural soil, *Global Change Biol.*, *6*, 303-316, 2000.
- Williams, E., D. Parrish, and F. Fehsenfeld, Determination of nitrogen oxide emissions from soils: Results from a grassland site in Colorado, U.S., *J. Geophys. Res.*, *92*, 2173-2179, 1987.

D.E. Rolston, Department of Land, Air, and Water Resources, University of California, One Shields Avenue, Davis, CA 95616. (derolston@ucdavis.edu.)

R.T. Venterea, Institute of Ecosystems Studies, Box AB, Millbrook, NY 12545. (venterear@ecostudies.org.)

(Received May 9, 1999; revised January 3, 2000; accepted January 10, 2000.)